AD-A286 385

ARMY RESEARCH LABORATORY

Quantum Chemical Study of Rare Gas/Halide Interactions as a Model for High Energy Density Material: II. The Interaction of Hydrogen Chloride With the Rare Gas Xenon

George F. Adams
Cary F. Chabalowski

ARL-TR-621 November 1994

94-35612

NOV 21 1994

APPROVED FOR PUBLIC RELEASE; DISTRIBUTION IS UNLIMITED

6

NOTICES

Destroy this report when it is no longer needed. DO NOT return it to the originator.

Additional copies of this report may be obtained from the National Technical Information Service, U.S. Department of Commerce, 5285 Port Royal Road, Springfield, VA 22161.

The findings of this report are not to be construed as an official Department of the Army position, unless so designated by other authorized documents.

The use of trade names or manufacturers' names in this report does not constitute indorsement of any commercial product

REPORT DOCUMENTATION PAGE

Form Approved
OMB No 0704-0188

Public reporting burden for this collection of information is estimated to average 1 hour per response, including the time for reviewing instructions, searching existing data sources, gathering and maintaining the data needed, and completing and reviewing the collection of information. Send comments regarding this burden estimate or any other aspect of this collection of information, including suggestions for reducing this burden, to Washington Headquarters Services, Directorate for Information Operations and Reports, 1215 Jefferson Davis Highway, Suite 1204, Arlington, VA 22202-4302, and to the Office of Management and Budget, Paperwork Reduction Project (0704-0188), Washington, DC 20503.

1. AGENCY USE ONLY (Leave blank)	2. REPORT DATE	3. REPORT TYPE AND DATES COVERED
	November 1994	Final, Sep 89–Sep 91

4. TITLE AND SUBTITLE

Quantum Chemical Study of Rare Gas/Halide Interactions as a Model for High-Energy Density Material: II. The Interaction of Hydrogren Chloride With the Rare Gas Xenon

5. FUNDING NUMBERS

PR: 1L161102AH43

6. AUTHOR(S)

George F. Adams and Cary F. Chabalowski

7. PERFORMING ORGANIZATION NAME(S) AND ADDRESS(ES)

U.S. Army Research Laboratory
ATTN: AMSRL-WT-PC
Aberdeen Proving Ground, MD 21005-5066

8. PERFORMING ORGANIZATION REPORT NUMBER

9. SPONSORING/MONITORING AGENCY NAME(S) AND ADDRESS(ES)

U.S. Army Research Laboratory
ATTN: AMSRL-OP-AP-L
Aberdeen Proving Ground, MD 21005-5066

10. SPONSORING/MONITORING AGENCY REPORT NUMBER

ARL-TR-621

11. SUPPLEMENTARY NOTES

12a. DISTRIBUTION/AVAILABILITY STATEMENT

Approved for public release; distribution unlimited.

12b. DISTRIBUTION CODE

13. ABSTRACT (Maximum 200 words)

Electronic transitions from laser excitation have produced charge transfer (CT) reactions in doped xenon solids, which in turn generate spatially separated, long-lived, dipolaron states. These quasi-stable separated charges have been proposed as an energy storage mechanism in the study of high-energy density materials. In a previous study, we performed calculations on selected singlet electronic states of HCl, and in this study we investigate the character of the low-lying singlet electronic states in the systems Cl + Xe and HCl + Xe. The results show at least one excited electronic state which is ionic in nature and could serve as a CT state. It is also known from experimentation that following excitation into the CT state, the H-Cl bond is ruptured. The CT state located in this study is described primarily by a molecular orbital with σ-antibonding character in the H-Cl bonding region. This CT state would therefore provide both a charge transfer mechanism and a means for weakening or breaking the H-Cl bond consistent with experimental observations. In this report, we also provide potential energy surfaces and electronic transition probabilities as a function of R(HCl•••Xe) for a linear arrangement.

14. SUBJECT TERMS

electronic states, charge transfer, high-energy density materials, rare gas (Rg)/halides, quantum chemistry

15. NUMBER OF PAGES

37

16. PRICE CODE

17. SECURITY CLASSIFICATION OF REPORT	18. SECURITY CLASSIFICATION OF THIS PAGE	19. SECURITY CLASSIFICATION OF ABSTRACT	20. LIMITATION OF ABSTRACT
UNCLASSIFIED	UNCLASSIFIED	UNCLASSIFIED	UL

INTENTIONALLY LEFT BLANK.

TABLE OF CONTENTS

		Page
	LIST OF FIGURES	v
	LIST OF TABLES	vii
1.	INTRODUCTION	1
2.	DETAILS OF CALCULATIONS	3
3.	Xe-Cl INTERACTIONS	4
3.1	Details of Configuration Interaction Calculations	4
3.2	Results	5
3.2.1	Neglecting Spin-Orbit	5
3.2.2	Including Spin-Orbit	5
4.	HCl-Xe INTERACTIONS	13
4.1	The B_1 States	15
4.1.1	The $1B_1$ State	15
4.1.2	The $2B_1$ State	18
4.1.3	The $3B_1$ State	21
4.2	The A_1 States	22
4.2.1	The $2A_1$ State	22
4.2.2	The $3A_1$ State	27
5.	CONCLUSIONS	28
6.	REFERENCES	29
	DISTRIBUTION LIST	33

Accession For
NTIS GRA&I
DTIC TAB
By
Dist
A-1

INTENTIONALLY LEFT BLANK.

LIST OF FIGURES

Figure		Page
1.	Potential energy curves (all units are atomic) for the $1,2(^2\Sigma^+)$ and $1,2(^2\Pi)$ electronic states in XeCl as a function of internuclear separation excluding spin-orbit effects	6
2.	Absolute value of the electric dipole transition moments, μ_e (in atomic units), for the strong transitions $2^2\Sigma^+ \leftarrow 1^2\Sigma^+$ and $2^2\Pi \leftarrow 1^2\Pi$ in XeCl as a function of internuclear separation	7
3.	Potential energy curves for six states of XeCl including the effects of spin-orbit interactions	10
4.	Potential energy curves for the x-component of the three lowest $^1\Pi$ electronic states belonging to the B_1 IRREP in linear HClXe	16
5.	Absolute value of the electric dipole transition moment, μ_e (in atomic units), for the transitions from the ground state to the x-component of the three lowest lying singlet Π states belonging to the B_1 IRREP	17
6.	Potential energy curves for the three lowest $^1\Sigma^+$ electronic states belonging to the A_1 IRREP in linear HClXe	23
7.	Potential energy curves for the $2A_1$ and $2B_1$ electronic states in linear HClXe	24
8.	Absolute value of the electric dipole transition moment, μ_e (in atomic units), for the transitions from the ground state to the two lowest lying $^1\Sigma^+$ excited states belonging to the A_1 IRREP	26

INTENTIONALLY LEFT BLANK.

LIST OF TABLES

Table		Page
1.	Molecular Constants and Radiative Lifetimes for XeCl Ignoring SO Effects	8
2.	Molecular Constants and Radiative Lifetimes for XeCl Including SO Effects	11
3.	Reference CSFs and Total Number of CSFs Used in Defining the Cl Wave Functions for HClXe	15
4.	Absolute Values of the Electric Dipole Transition Moments, μ_e, Between the Ground $\tilde{X}(^1A_1)$ and Excited States at Selected R(HCl•••Xe) Distances	19
5.	Permanent Electric Dipole Moments at Selected R Values for the Six Electronic States in This Study	19
6.	Vertical Transition Energies, T, Between the Ground $\tilde{X}(^1A_1)$ and Excited States at Selected R(HCl•••Xe) Distances	20
7.	Calculated D_e's for HClXe[a]	25

INTENTIONALLY LEFT BLANK.

1. INTRODUCTION

In our initial study of rare gases (Rg), we examined the possibility of storing energy for extended periods in the $a^3\Sigma_u^+$ excited electronic state of the helium dimer (Chabalowski et al. 1988). Our calculations provided the first reliable estimate of the lifetime of this state, which was found to be 18 s for the isolated dimer. We are continuing to explore the possibilities of using the Rg as a medium for high-energy density storage.

Apkarian and coworkers (Fajardo and Apkarian 1986, 1988a, 1988b) have chosen solids composed of Rg atoms as a starting point for studying energy storage via photo-induced, charge transfer (CT) reactions. This choice was based, in part, upon the Rg atoms providing " . . . the necessary conceptual simplicity to afford a detailed and rigorous description of the fundamentals of these processes." Part of this "simplicity" is due to the absence of complex ground state interactions. Apkarian et al. have studied spectra of these CT transitions in liquid xenon (Wiedeman, Fajardo, and Apkarian 1987; Okada, Wiedeman, and Apkarian 1989; Fajardo et al. 1988) and in doped Rg solids (Fajardo and Apkarian 1986, 1988a, 1988b, 1987; Kunttu et al. 1990; Okada, Wiedeman, and Apkarian 1989) (for various Rg systems) demonstrating that spatially separated, long-lived, dipolaron states are produced in the Xe/Cl system via the reaction (Fajardo and Apkarian 1988b):

$$Xe + HCl + 2h\nu \rightarrow Xe^{+}(HCl)^{-}.$$

In addition, they have demonstrated the lasing capabilities of XeF in crystalline argon, creating a laser tunable over an 80-nm range in the visible region (Katz, Feld, and Apkarian 1989). Other combination of Rg halides are expected to be likely candidates as tunable lasers in the visible, ultraviolet (UV), and vacuum UV spectral regions (Schwentner and Apkarian 1989). Classical molecular dynamics studies by Gerber and coworkers (Gerber, Alimi, and Apkarian 1989; Alimi, Brokman, and Gerber 1989; Alimi, Gerber and Apkarian 1989) have shed some light on possible mechanisms for dissociating F_2 (Alimi, Gerber, and Apkarian 1990), Cl_2 (Gerber, Alimi, and Apkarian 1989; Alimi, Brokman, and Gerber 1989), and HI (Alimi, Gerber, and Apkarian 1989) in Rg solids. They found large qualitative differences in the dissociation mechanisms as well as the dynamical pathways followed by the dissociated atoms among these three molecules.

Last and George (LG) (Last and George 1987a, 1987b, 1988; Last, Kim, and George 1987; Last et al. 1987) have performed semi-empirical (i.e., DIM and DIIS) quantum chemical calculations on various (Xe, Cl) and (Xe, HCl) systems, predicting potential energy surfaces, permanent dipole moments, electronic transition energies, and electric transition dipole moments. From these calculations, they made assignments to the observed absorption and emission spectra, provided structural data for the complexes in the gas and solid states, and rationalized the observed bandwidths. Their findings are generally in good qualitative agreement with experiment. As LG have pointed out, there have been very few ab initio calculations on related systems.

With respect to energy storage, the physical model for the long-lived, separated charges is a halide negative ion separated from the trapped, positively charged hole state which appears to be quasi-localized on Rg molecules of weakly bound Rg atoms. There is evidence suggesting that the positively charged $Rg_n(+)$ chains are linear and prefer n=3 in the solids (Fajardo and Apkarian 1988b), with the Rg-Rg interatomic distance being shorter than what is seen in the neutral Rg matrix. These separated dipolaron states can exist so long as the negatively charged halide, X(-), remains separated from the $Rg_n(+)$ hole. But when the (+) holes migrate to the X(-), they rapidly form the exciplex $Xe_2(+)X(-)$, releasing the exciton energy as fluorescence. The gas phase equilibrium geometry for the Xe_2Cl exciplex in the $4^2\Gamma$ state is predicted to have a Xe-Xe separation of 3.17 Å (5.99 bohr) (Stevens and Krauss 1982) and a Cl-Xe separation of 6.41 bohr (Fajardo and Apkarian 1986).

The cationic self-trapped holes (STHs) can migrate to the X(-) by one of the following two methods: (1) either by tunneling, or (2) by "hopping" (Fajardo and Apkarian 1988b) (due to a thermal perturbation) which stretches the $Xe\text{-}Xe_n(+)$ bond lengths to the neutral geometry, apparently increasing the energy of the $Rg_n(+)$ to that of an excited hole state and conducting the hole to the X(-). At a constant temperature of 12 K, the separated dipolarons for Cl in Xe have been shown to exist for longer than 30 hr, with the rate-determining step to recombination being the ability of the trapped hole to tunnel (Fajardo and Apkarian 1988b).

Schwentner, Fajardo, and Apkarian (1989) presented the CT process as the excitation of a positive "hole" (analogous to an electron in an atom) into a Rydberg orbit with the halide atom acting as a negatively charged "nucleus" of infinite mass. Based on this model, they calculate the Rydberg term values B_n and the state radii r_n for these Rydberg states. The progression of predicted B_n energies fit quite nicely to the experimentally derived values obtained from excitation spectra. To date, Xe has been the

only Rg+halide matrix to show such a Rydberg (hole) progression spectra (Schwentner, Fajardo, and Apkarian 1989). This delocalized Rydberg "hole" description has been shown to be applicable for Xe and perhaps Kr but not the lighter Rg atoms (Schwentner, Fajardo, and Apkarian 1989). In addition, no evidence has been seen experimentally to support a delocalized hole state for F in Rg solids. Xe appears to play a special role among the Rg in its ability to stabilize the charge separation. This dependence of the charge transfer process and stabilization on the halogen and type of Rg matrix warrants further theoretical study.

To obtain an understanding of the microscopic processes involved in formation of the exciplex, as well as the factors determining the lifetime of the separated dipolarons, one needs detailed information about the electronic structure and molecular interactions. This report describes an ab initio study of the Rg/halide interactions of HCl with Xe atoms. Extending our previous work on HCl (Adams and Chabalowski, to be published), quantum chemical calculations are performed on the ground and low lying excited states of XeCl and HClXe, using effective core potentials (ECPs) to represent the inner shell electrons, state-averaged complete active space MCSCF (SA-CASSCF), and configuration interaction (CI) calculations. The purpose for the XeCl calculations was to ascertain how well the ECPs reproduce known experimental molecular properties as well as properties calculated by earlier ab initio studies. In the HClXe system, we are most interested in determining the qualitative nature of the excited electronic states and if a CT state exists even in these small model systems. The permanent electric dipole moments and transition dipole moments will also be predicted as a function of HClXe separation. The transition moments offer a semi-quantitative measure for the likelihood of populating each electronic state.

2. DETAILS OF CALCULATIONS

All calculations were carried out in the C_{2v} point group. The atomic basis sets used are a combination of Gaussian-type orbitals and the ECPs of Wadt and Hay (1985). The ability of our codes to handle ECPs allows for the treatment of systems including such heavy atoms as Xe. The Guassian basis consists of an uncontracted set of four s-type primitives (Van Duijneveldt 1971) and one p-type polarization function (σ_p=0.75) on hydrogen, giving [4s,1p]. The chlorine basis contains three noncontracted s- and p-type valence atomic obitals (AOs) with exponents optimized for their use with the ECPs (Wadt and Hay 1985). This is augmented by a negative ion function (σ_p=0.049) (Dunning and Hay 1977) and a polarization function (σ_d=0.50) (Dunning and Hay 1977), as well as a set of noncontracted Rydberg functions (σ_s=0.025, σ_p=0.020, σ_d=0.015) (Dunning and Hay 1977), for a total basis set of [4s,5p,2d]. Likewise,

the Xe basis associated with the ECPs (Wadt and Hay 1985) consists of three s- and p-type primitives which remained uncontracted and were augmented by a single polarization function (σ_d=0.25) (Hay and Dunning 1978), giving [3s,3p,1d].

The molecular orbitals (MOs) used as expansion vectors in the CI calculations are obtained from the SA-CASSCF calculations using the general second-order density matrix driven MCSCF algorithm of Lengsfield (1982). These MOs should be suitable for describing both the ground and excited states. The CI wavefunctions are generated from the symbolic matrix element, direct-CI method called ALCHEMY (Liu and Yoshimine 1981) by doing all single and double electronic excitations from a set of reference configuration state functions (CSFs). The details of the SA-CASSCF and CI approaches will be given in the appropriate sections.

Potential energy curves (PECs) and electronic transition dipole moments are then calculated as a function of atomic positions. The vibrational wavefunctions corresponding to the PECs for the diatomic systems were determined by solving the radial Schroedinger equation for nuclear motion (ignoring rotational motion). Transition probabilities and radiative lifetimes are predicted based upon the previously mentioned treatment. One potential weakness in these calculations is the neglect of spin-orbit (SO) interactions. But earlier theoretical work done by Hay and Dunning (1978) on XeCl showed that much useful qualitative and semi-quantitative information can be obtained without inclusion of SO effects.

3. Xe-Cl INTERACTIONS

3.1 Details of Configuration Interaction Calculations. We have calculated the PECs for the $1,2^2\Sigma^+$ and the $1,2^2\Pi$ states. In the C_{2v} point group these states transform as $\Sigma^+(A_1)$, $\Pi_x(B_1)$, and $\Pi_y(B_2)$, so the state symmetries included in the SA-CASSCF are $1,2A_1$, $1,2B_1$, and $1,2B_2$, with the weighing scheme w=(1,1,1,1,1,1). Due to the molecular symmetry, no loss of generality occurs by considering only the x-component of the Π states in the CIs, with an appropriate factor of 2 applied when necessary. All the valence electrons remained active in the CI, and the entire set of virtual orbitals was retained. The MO fillings in the two reference CSFs for the $^2\Sigma^+(A_1)$ states are $(1\sigma^2,2\sigma^2,3\sigma^2,4\sigma^1,1\pi_x^2,1\pi_y^2,2\pi_x^2,2\pi_y^2)$ and $(1\sigma^2,2\sigma^2,3\sigma^1,4\sigma^2,1\pi_x^2,2\pi_y^2,2\pi_x^2,2\pi_y^2)$, and for the $^2\Pi_x(B_1)$ states are $(1\sigma^2,2\sigma^2,3\sigma^2,4\sigma^2,1\pi_x^2,1\pi_y^2,2\pi_x^1,2\pi_y^2)$ and $(1\sigma^2,2\sigma^2,3\sigma^2,4\sigma^2,1\pi_x^1,1\pi_y^2,2\pi_x^2,2\pi_y^2)$. All single and double excitations were done from these filled orbitals into the virtual space.

The final CI wavefunctions are then used to study the strong transitions $2^2\Pi \rightarrow 1^2\Pi$ and $2^2\Sigma^+ \rightarrow 1^2\Sigma^+$, as well as the weak $2^2\Pi \rightarrow 1^2\Sigma^+$ and $2^2\Sigma^+ \rightarrow 1^2\Pi$ transitions, reporting lifetimes for emissions from the v'=0 levels. This is believed to be the first report of theoretical predictions for the lifetimes of the weak transitions. Empirical spin-orbit (SO) effects are then included to obtain SO-corrected PECs and electric dipole transition moments for three transitions.

3.2 Results.

3.2.1 Neglecting Spin-Orbit. The X Cl system has already been studied both theoretically (Hay and Dunning 1978; Huber and Herzberg 1979) and experimentally (Inoue, Ku, and Setser 1984; Grieneissen, Xue-Ting, and Komps 1981; Velazco and Setser 1975; Brau and Ewing 1975). The current PECs without SO effects can be seen in Figure 1, and molecular constants are reported in Table 1 along with values from theoretical work by Hay and Dunning (1978) (HD) and available experimental values. As can be seen in Table 1, our equilibrium bond lengths and ω_e's are in reasonably good agreement with HD's values. Figure 2 gives the electric dipole transition moments, μ_e, for the strong transitions as a function of R(Xe-Cl). Near the R_e(6.4 bohr) for the 2 $^2\Sigma^+$ excited state, the ω_e for the Σ-Σ transition is approximately 4.5 times greater than the Π-Π moment. The transition moments and PECs from this work are nearly identical to those calculated by HD when SO is ignored.

Table 1 also includes the results of our vibrational analysis for the radiative lifetimes. Again, our predicted lifetimes for the strong transitions, $\tau(2^2\Sigma^+ \rightarrow 1^2\Sigma^+)$=6.0 ns and $\tau(2^2\Pi \rightarrow 1^2\Pi)$=74.0 ns, are very similar to HDs without SO effects (i.e., 5.6 ns and 64.0 ns, respectively). In HD's study, the SO corrections had a significant affect on these lifetimes, nearly doubling the aforementioned values.

3.2.2 Including Spin-Orbit. It should be kept in mind that with the inclusion of SO effects, the term symbols $^2\Sigma^+$ and $^2\Pi$ will only be approximations to the correct state descriptions due to mixing of different Λ components of Ω through the spin-orbit operator. We have included SO couplings in the same way as HD, using the empirically obtained atomic Cl and Xe^+ SO coupling parameters. The inclusion of SO effects mixes the $2^2\Pi$-$2^2\Sigma^+$ and $1^2\Pi$-$1^2\Sigma^+$ states. The resulting wavefunctions for the states, in HD's nomenclature, are as follows:

with Ω=1/2,

$$I_{1/2}(1^2\Sigma^+) = A_{COV}\Psi^0(1^2\Sigma^+\alpha) + B_{COV}\Psi^0(1^2\Pi\beta) = \tilde{X}, \qquad (1)$$

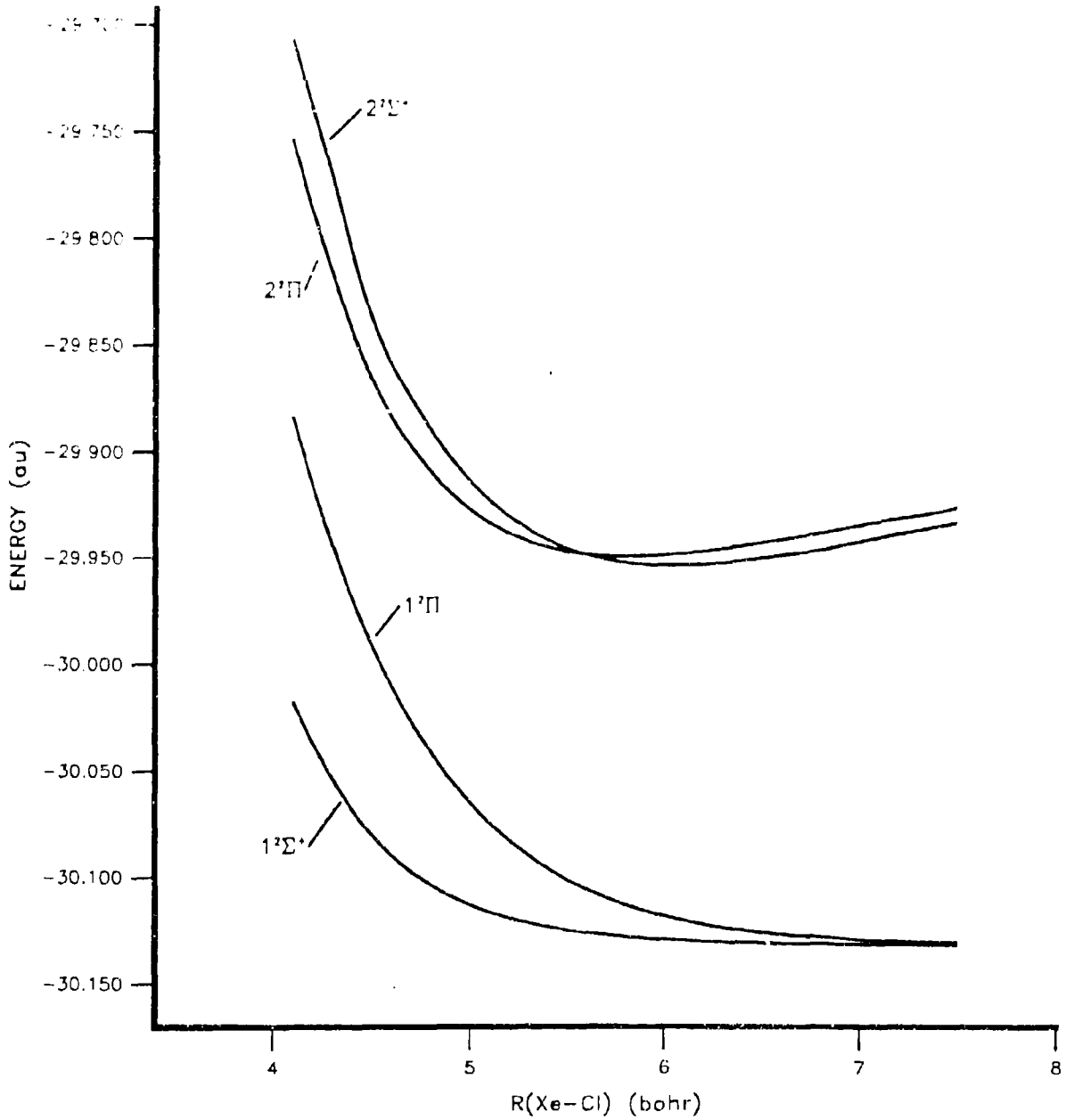

Figure 1. Potential energy curves (all units are atomic) for the 1,2($^2\Sigma^+$) and 1,2($^2\Pi$) electronic states in XeCl as a function of internuclear separation excluding spin-orbit effects.

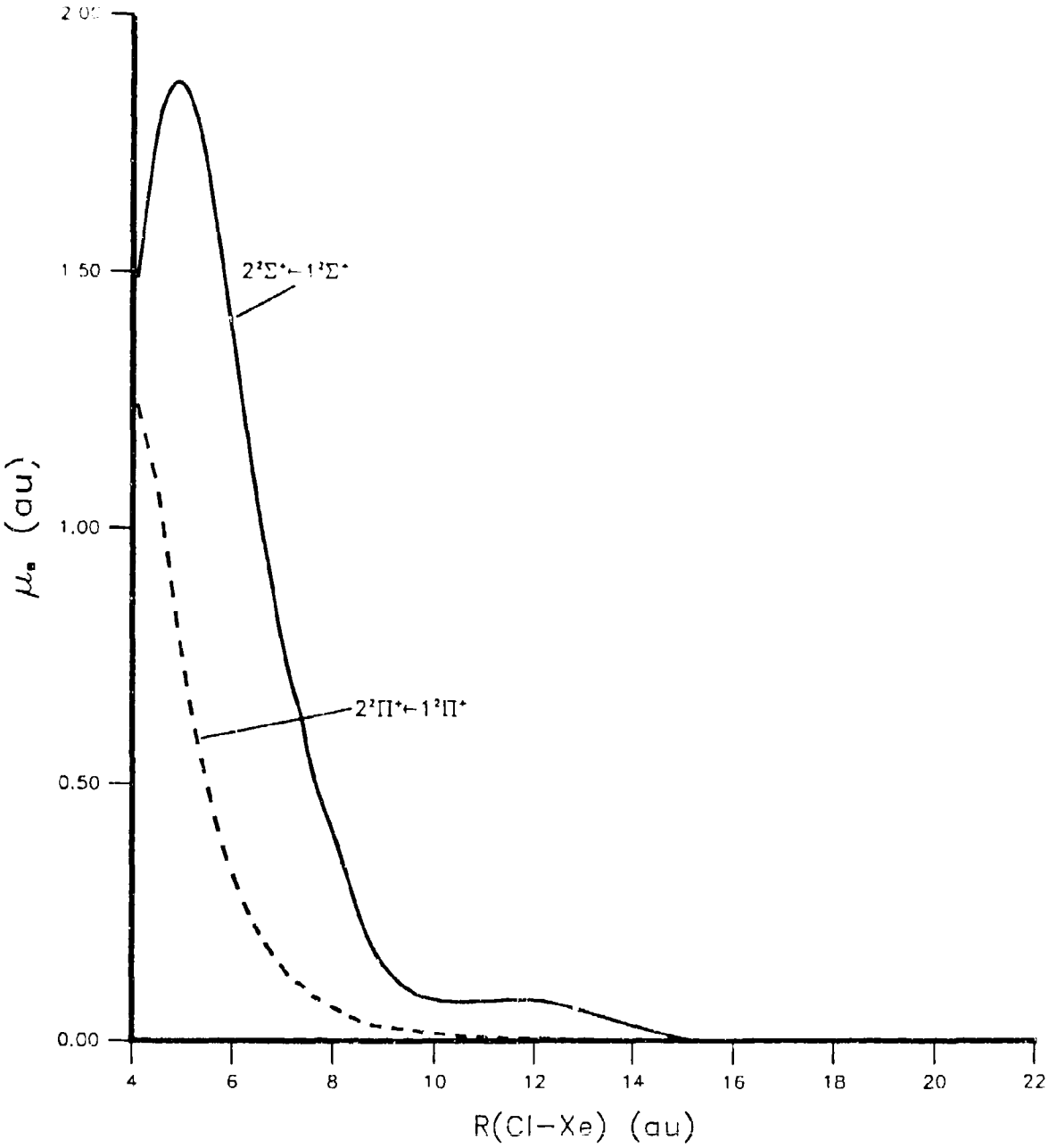

Figure 2. Absolute value of the electric dipole transition moments, μ_o (in atomic units), for the strong transitions $2^2\Sigma^+ \leftarrow 1^2\Sigma^+$ and $2^2\Pi \leftarrow 1^2\Pi$ in XeCl as a function of internuclear separation.

Table 1. Molecular Constants and Radiative Lifetimes for XeCl Ignoring SO Effects

	R_e(Å)		ω_e(mv^{-1})	
State	HERE	HD[a]	HERE	HD
$2^2\Sigma^+$	3.20	3.25	198.0	190.0
$2^2\Pi$	3.08	3.14	196.0	188.0

	Radiative Lifetimes (ns)		
TRANSITION	HERE	HD	EXPERIMENT
$2^2\Sigma^+ - 1^2\Sigma^+$	6.0	5.6	11.1[b],17.0[c]
$2^2\Pi - 1^2\Pi$	74.0	64.0	131.0[b],53.0[c]
$2^2\Pi - 1^2\Sigma^+$	13.0 μs		
$2^2\Sigma^+ - 1^2\Pi$	50.0 μs		

[a] Okada, Wiedeman, and Apkarian (1989).
[b] Fajardo et al. (1988).
[c] Wadt and Hay (1985); Hay and Dunning (1978).

$$II_{1/2}(1^2\Pi) = -B_{COV}\Psi^0(1^2\Sigma^+\alpha) + B_{COV}\Psi^0(1^2\Pi\beta), \tag{2}$$

$$III_{1/2}(2^2\Sigma^+) = A_{ion}\Psi^0(2^2\Sigma^+\alpha) + B_{ion}\Psi^0(2^2\Pi\beta) = \tilde{B}, \tag{3}$$

and

$$V_{1/2}(2^2\Pi) = -B_{ion}\Psi^0(2^2\Sigma^+\alpha) + B_{ion}\Psi^0(2^2\Pi\beta). \tag{4}$$

With Ω=3/2,

$$I_{3/2}(1^2\Pi) = \Psi^0(1^2\Pi) = \tilde{A}, \tag{5}$$

and

$$II_{3/2}(2^2\Pi) = \Psi^0(2^2\Pi) = \tilde{C}, \tag{6}$$

where $\Psi^1(1^2\Pi;1^2\Sigma^+)$ designates the correction to the $1^2\Sigma^+$ state due to the SO interaction with the $1^2\Pi_{1/2}$ state. Within this four-state (in zeroth-order) model, the $\Psi^0(1^2\Pi_{3/2})$ and $\Psi^0(2^2\Pi_{3/2})$ components of the Π states have no other spin states with which to couple, so the energies of the $I_{3/2}$ and $II_{3/2}$ have been SO "corrected" by HD (and here) according to the following simple formulae used by HD:

$$E(I_{3/2}) = E(1^2\Pi) - \lambda_{Cl}, \tag{7}$$

and

$$E(II_{3/2}) = E(2^2\Pi) - \lambda_{XE+}, \tag{8}$$

where λ_{Cl}=294 cm^{-1} and λ_{Xe+}=3,512 cm^{-1} are the atomic SO coupling constants for the Cl and Xe^+ atoms, respectively. These values were taken from HD's Table II and assumed to be independent of internuclear separation. The mixing coefficients A and B, as well as the energies for the Ω=1/2 states, are obtained by diagonalizing the 2x2 matrices as follows:

$$\begin{bmatrix} E(^2\Sigma^+) & -\sqrt{2}\lambda_x \\ -\sqrt{2}\lambda_x & E(^2\Pi)+\lambda_x \end{bmatrix}.$$

The λ_x is either λ_{Cl} (for the covalent states) or λ_{Xe+} (for the ionic states). The λ is defined as the SO splitting parameter,

$$\lambda = \frac{\left[E(^2P_{1/2} - E(^2P_{3/2})\right]}{3}. \tag{9}$$

Figure 3 shows the PECs for the six states represented by Equations 1–6 with SO corrections to the energies included as described previously.

The R_e and ω_e for a selection of SO-corrected states are given in Table 2. It can be seen that the SO correction has had little effect on the R_e and ω_e values for the $III_{1/2}$ and $IV_{1/2}$ states. Once again, our results for R_e and ω_e are seen to be very similar to those of HD when SO is included, with the current values lying slightly closer to experiment than HD's. For the $III_{1/2}$ state, our R_e and ω_e values are 3.17 Å

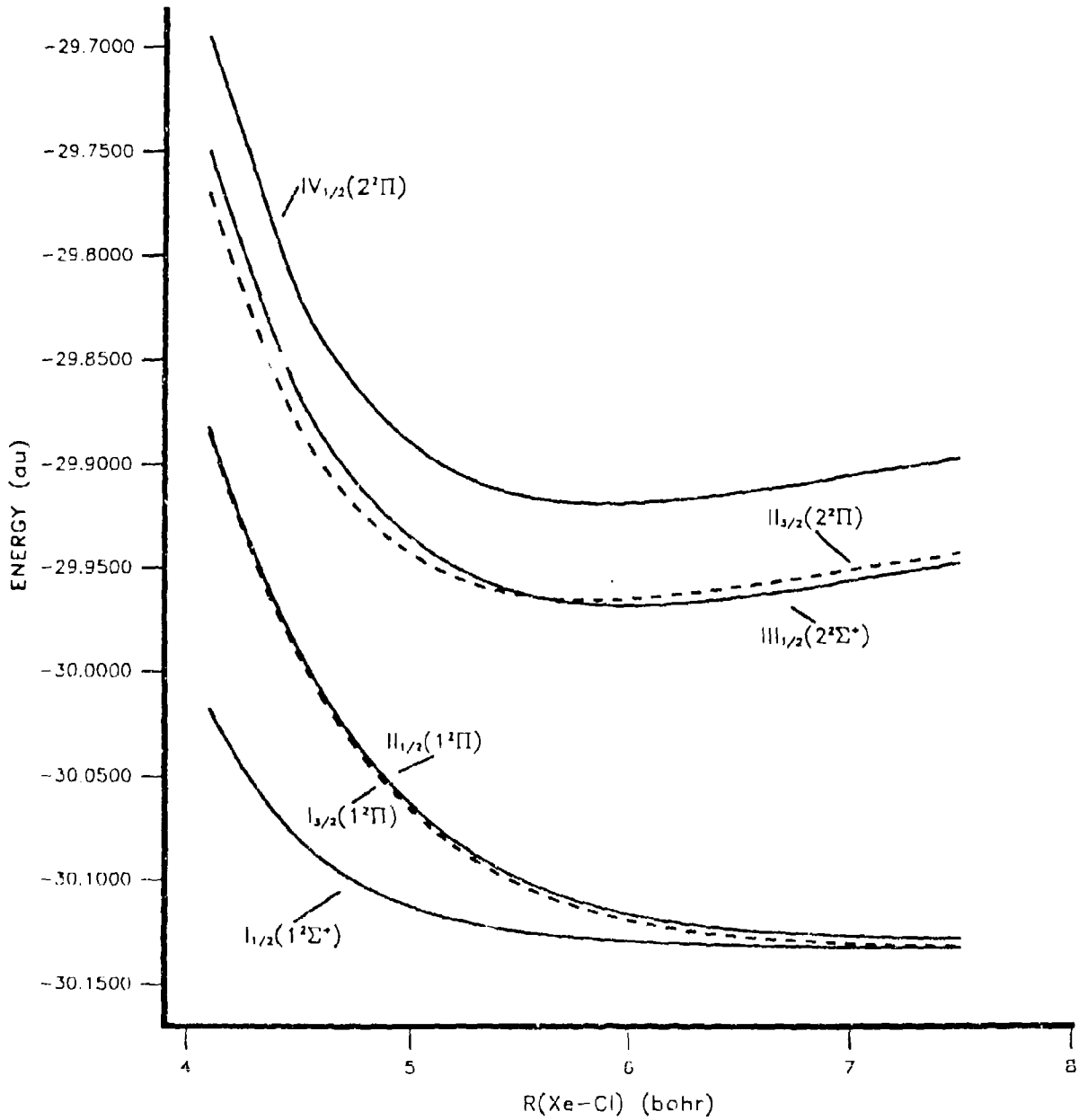

Figure 3. Potential energy curves for six states of XeCl including the effects of spin orbit interactions. (See the text in Section 3.2.2 for a detailed description of the electronic states).

Table 2. Molecular Constants and Radiative Lifetimes for XeCl Including SO Effects

State	R_e(Å) HERE	R_e(Å) HD[a]	R_e(Å) Exp.[b]	ω_e(cm^{-1}) HERE	ω_e(cm^{-1}) HD	ω_e(cm^{-1}) Exp.[b]
$III_{1/2}$	3.17	3.22	2.94	195.0	188.0	195
$IV_{1/2}$	3.12	3.18	—	198.0	189.0	—

Transition Moments (μ_e) and Radiative Lifetimes (τ)

Transition	HERE μ_e[f]	HERE τ[g]	HD μ_e	HD τ	Experiment τ
$III_{1/2} \rightarrow I_{1/2}$	2.97	8.0	2.75	11.0	11.1,[c] 27.0[d]
$III_{3/2} \rightarrow I_{3/2}$	0.98	95.0	0.96	120.0	131.0,[c] 53.0[d]
$IV_{1/2} \rightarrow II_{1/2}$	0.49	168.0	0.50	180.0	—

ΔE(eV)

Transition	HERE	HD	Experiment
$III_{1/2} \rightarrow I_{1/2}$	4.39	4.20	4.03[e]
$III_{3/2} \rightarrow I_{3/2}$	4.05	3.76	3.63[c]
$IV_{1/2} \rightarrow II_{1/2}$	5.32	5.13	—

[a] Okada, Wiedeman, and Apkarian (1989).
[b] Inoue, Ku, and Setser (1984).
[c] Fajardo et al. (1988).
[d] Liu and Yoshimine (1981).
[e] Wadt and Hay (1985); Hay and Dunning (1978).
[f] μ_e in units of Debye.
[g] τ in units of ns.

and 195 cm^{-1}, respectively. The corresponding experimental values are 2.94 Å and 195 cm^{-1}. HD's values are 3.22 Å and 188 cm^{-1}, respectively. This similarity between the results from our study and from HD's is expected due to the nearly identical results obtained between the two studies before including SO effects.

The electric dipole transition moments over SO states are as follows:

$$<III_{1/2}|\mu_e|I_{1/2}> = A_{COV}A_{ION}<\Psi^0(2^2\Sigma^+)> + B_{COV}B_{ION}<\Psi^0(2^2\Pi)|\mu_e|\Psi^0(1^2\Pi)>, \quad (10)$$

$$<IV_{1/2}|\mu_e|II_{1/2}> = -A_{COV}B_{ION}<\Psi^0(2^2\Sigma^+)|\mu_e|\Psi^0(1^2\Sigma^+)> + B_{COV}A_{ION}<\Psi^0(2^2\Pi)|\mu_e|\Psi^0(1^2\Pi)>, \quad (11)$$

and

$$<II_{3/2}|\mu_e|I_{3/2}> = <\Psi^0(2^2\Pi)|\mu_e|\Psi^0(1^2\Pi)>. \quad (12)$$

The results for the radiative lifetimes (including SO) are also given in Table 2. The transition dipole moments and ΔEs were taken in this study near the minima for the excited states. These are R=5.80 bohr for the $II_{3/2}$, R=5.90 bohr for the $IV_{1/2}$, and R=6.00 for the $III_{1/2}$ state. The lifetime, τ, is calculated from the definition of the Einstein coefficient for spontaneous emission;

$$A = \frac{1}{\tau} = 1.063\ (\mu_{ij})^2(\Delta E)^3 \times 10^6\ \text{sec}^{-1}. \quad (13)$$

For the $III_{1/2}\rightarrow I_{1/2}$ transition, the lifetimes are τ-(8 ns;11 ns;11 ns [Inoue, Ku, and Setser 1984], and 27 ns [Grieneissen, Xue-Ting, and Komps 1981]) with the order being (1) this study; (2) HD; and (3) experiments, respectively. The lifetimes for the $II_{3/2}\rightarrow I_{3/2}$ transition are (95 ns;120 ns;131 ns [Inoue, Ku, and Setser 1984], and 53 ns [Grieneissen, Xue-Ting, and Komps 1981]), and for the $IV_{1/2}\rightarrow II_{1/2}$ τ=(168ns; 180ns; no experiment). For the $III_{1/2}\rightarrow I_{1/2}$ lifetime, the current result and that of HD's are in good agreement with the more recent experiments of Inoue, Ku, Setser (1984). The lifetime for the $II_{3/2}\rightarrow I_{3/2}$ transition from this study lies midway between the two experimental values and 21% smaller than the theoretical value predicted by HD. The agreement between the two theoretical studies is much better for the $IV_{1/2}\rightarrow II_{1/2}$ transition (no experimental data available), where our τ is only 7% smaller than HD's.

The discrepancy between the current $\tau(II_{3/2}\rightarrow I_{3/2})$ value and that of HD is due in part to a significantly larger ΔE predicted in the current study. Table 2 lists the three transition energies predicted by the two theoretical studies, as well as the experimental values for the $III_{1/2}\rightarrow I_{1/2}$ and $II_{3/2}\rightarrow I_{3/2}$ transitions. This study predicts $\Delta E(II_{3/2}\rightarrow I_{3/2})$=4.05 eV, while HD predicts 3.76 eV, which is closer to the experimental value of 3.63 eV. As a general statement, the level of CI theory used in the current study should be able

to generate more accurate wave functions than the correlation techniques used by HD. Apparently, the higher-lying state in this study did not receive the same level of correlation corrections as the lower state, even though each wave function could very well be a better description of that respective electronic state than what was produced in the CI calculations of HD.

Since experimental ΔEs are usually fairly accurately known, one commonly used technique to predict a lifetime from theory is to combine the theoretical value for the transition dipole moment with the experimental ΔE, thus eliminating the uncertainty in τ due to the transition energy. If we recalculate the lifetimes for this study and HD's study using this technique, we get τ=133 ns from this study and τ=138 ns from HD, using the electric dipole transition moments from Table 2. These are both very close to the experimental value of 131 ns predicted by Inoue et al., with the current study now being in better agreement with experiment than HD's value. The τ's for the $III_{1/2} \rightarrow I_{1/2}$, recalculated in this fashion, are τ(this study)=10.4 ns and τ(HD)=12.1 ns, to be compared with τ(exp.)=11.1 ns. This again puts our value of τ in better agreement with experiment than HD's value, although the agreement with experiment is quite satisfactory in both cases.

These calculations have shown that using effective core potentials, along with modest-sized single-and-double excitation CI wave functions, one can predict electronic transition probabilities in good agreement with the experimental values. This lends credence to the prediction of such values for electronic transitions in which experimentation has been unable to determine the lifetimes in these doped Rg systems.

4. HCl-Xe INTERACTIONS

HCl-Xe is treated as a linear system with the Xe opposite the hydrogen atom. The atoms are coincidental with the z-axis of the global coordinate system. Calculations were performed at Cl-Xe separations of R(HCl-Xe)=(4.0,5.0,6.0,6.4,7.0,8.0,10.0,12.0,14.0,16.0,18.0,20.0,26.0) bohr while holding the H-Cl bond length at R_e=2.409 bohr (Huber and Herzberg 1979). Henceforth, R(HCl-Xe) will simply be referred to as R. All units are atomic unless otherwise stated. The calculations again use effective core potentials on Xe and Cl for all but the outer shell electrons. MOs are obtained at each point along the PEC from SA-CASSCF calculations averaging six electronic states (i.e., the two lowest energy roots from the A_1, B_1, and B_2 IRREPs). The ground state $\tilde{X}(\Sigma^+)$ transforms as the A_1 IRREP and the two Π components, (Π_x,Π_y) as the (B_1,B_2) IRREPs, respectively. A frozen core which included the two lowest

energy MOs of A_1 symmetry was maintained. The numbers of active MOs per IRREP were then (A_1=4,B_1=2,B_2=2,A_2=0), with the active electrons per IRREP being (A_1=4,B_1=4,B_2=4,A_2=0).

The use of ECPs is analogous to having a frozen core of MOs, so it must be kept in mind that the symmetry designations $1a_1$, $1b_1$, etc., for the MOs label the lowest energy, noncore MOs from the a_1, b_1,...IRREPs. With no further freezing of orbitals, these state-averaged MOs are used as expansion vectors in multireference, single-and-double excitation CI calculations at each point along the PECs. In the CIs, due to the axial symmetry of the system, only the $\Pi_x(B_1)$ component of the Π states is calculated. Three states were calculated from the A_1 IRREP and four states from the B_1. Three reference CSFs of A_1 symmetry were used and four of B_1 symmetry. The reference CSFs are listed in Table 3, along with the total number of CSFs retained per IRREP. Since only singlet states are treated in this study, the spin multiplicity label will be dropped from the state labels.

The typical means for describing the general characteristics of electronic states generated in CI calculations is to refer to the nature of the singly occupied MOs in the main CSFs for each state. This is especially useful in determining whether an electronic state is Rydberg, valence, or some mixture of these characters. But using state-averaged CASSCF MOs means that these orbitals, at least the ones included in the active space, are usually guaranteed to be some Rydberg-valence mixture if the states being averaged are of both characters, as it appears to be in this study. The fact that the state-averaged MOs are designed to simultaneously describe several states reduces somewhat their interpretive capabilities. Thus, apart from the following general comments regarding the MOs, the electronic states will be discussed primarily in terms of their calculated properties.

The A_1 states are described in their main CSFs by exciting a single electron from the $\sigma(4a_1)$ into either the $5a_1$ or $6a_1$ σ^* virtual MOs. The B_1 states are described by an excitation from either the $\pi(1b_1)$ bonding or $\pi(2b_1)$ antibonding MOs into either the $5a_1$ or $6a_1$ σ^* MOs. Therefore, both the $\Sigma(A_1)$ and $\Pi_x(B_1)$ use the same $\sigma^*(5a_1, 6a_1)$ virtual MOs, which are mixed Rydberg-valence in character for all values of R. At R=26.0, the $5a_1$ becomes essentially a Cl Rydberg-s orbital, and the $6a_1$ a HCl σ-antibonding orbital. In addition, the $\sigma(4a_1)$ MO, which is doubly occupied in the ground state, is almost entirely described by Xe atomic p_z orbitals for most R values. At the very short distances where R=(4.0,5.0), there is moderate contribution from the Cl s- and p-type AOs, but the Xe AOs are still dominant even at these close distances. So both the $2A_1$ and $3A_1$ electronic states arise primarily from an electronic excitation out of atomic Xe. All the R_e's reported here are determined from a simple three-point fit to a parabola.

Table 3. Reference CSFs and Total Number of CSFs Used in Defining the CI Wave Functions for HClXe

	Orbital Occupancies in Reference CSFs											
IRREPS	$1a_1$	$2a_1$	$3a_1$	$4a_1$	$5a_1$	$6a_1$	$1b_1$	$2b_1$	$3b_1$	$1b_2$	$2b_2$	$3b_2$
A_1 States	2	2	2	2	0	0	2	2	0	2	2	0
	2	2	2	1	1	0	2	2	0	2	2	0
	2	2	2	1	0	1	2	2	0	2	2	0
Total CSFs - 80,372												
B_1 States	2	2	2	2	1	0	2	1	0	2	2	0
	2	2	2	2	1	0	1	2	0	2	2	0
	2	2	2	2	0	1	2	1	0	2	2	0
	2	2	2	2	0	1	1	2	0	2	2	0
Total CSFs - 115,344												

4.1 The B_1 States. The four reference CSFs (see Table 3) for the $1,2,3^1B_1$ states represent $\pi \rightarrow \sigma^*$ excitations. As discussed previously, the open shell MOs in the main CSFs are a Rydberg-valence mixture and are more correctly referred to as diffuse orbitals rather than pure valence or Rydberg. In addition, the $6a_1$ MO is comprised primarily of AOs on HCl for R=(4.0,5.0,6.0), with increasing Xe character going from 5.0 to 8.0, at which point the $6a_1$ MO is essentially an even mix of HCl and Xe AOs. The $1b_1$ and $2b_1$ MOs are π bonding and antibonding in character, respectively. For $7.0 \leq R \leq 12.0$, all four MOs have significant contributions from AOs on both Cl and Xe, making the three B_1 states truly states of the complex and not isolated to either HCl or Xe within this range. Figure 4 contains the PECs for the electronic states of B_1 symmetry. It appears that the electronic states undergo significant changes in their character around R=16.0 bohr and again around 20.0 bohr. Figure 5 shows the absolute value of the electric dipole transition moments, μ_e, for the $1,2,3B_1 \leftarrow \tilde{X}$ transitions as a function of R(HCl-Xe). These too suggest major changes taking place in the description of the electronic states around 16.0 and 20.0 bohr.

4.1.1 The $1B_1$ State. The R_e for this state is predicted to lie at 8.98 bohr, which is 0.62 bohr longer than the ground state minimum. Figure 5 shows the transition moment for $1^1B_1 \leftarrow 1^1A_1$ changing rapidly going from R=4.0 to R=6.0 bohr. The transition moment starts out at 0.21 for R=4.0, then apparently

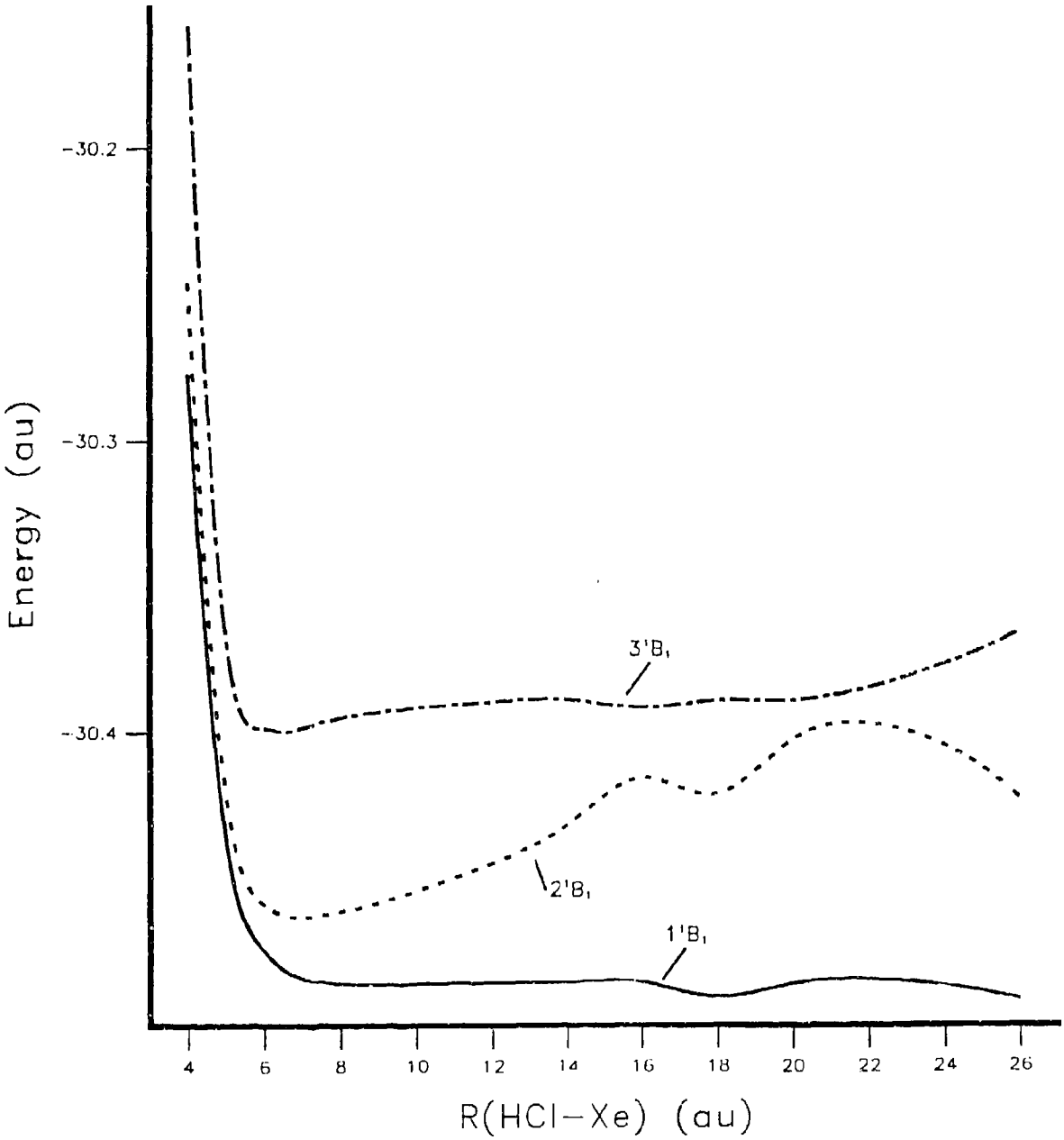

Figure 4. Potential energy curves for the Λ-component of the three lowest $^1\Pi$ electronic states belonging to the B_1 IRREP in linear HClXe. (See the text in section 4.1 for a detailed discussion of these states.)

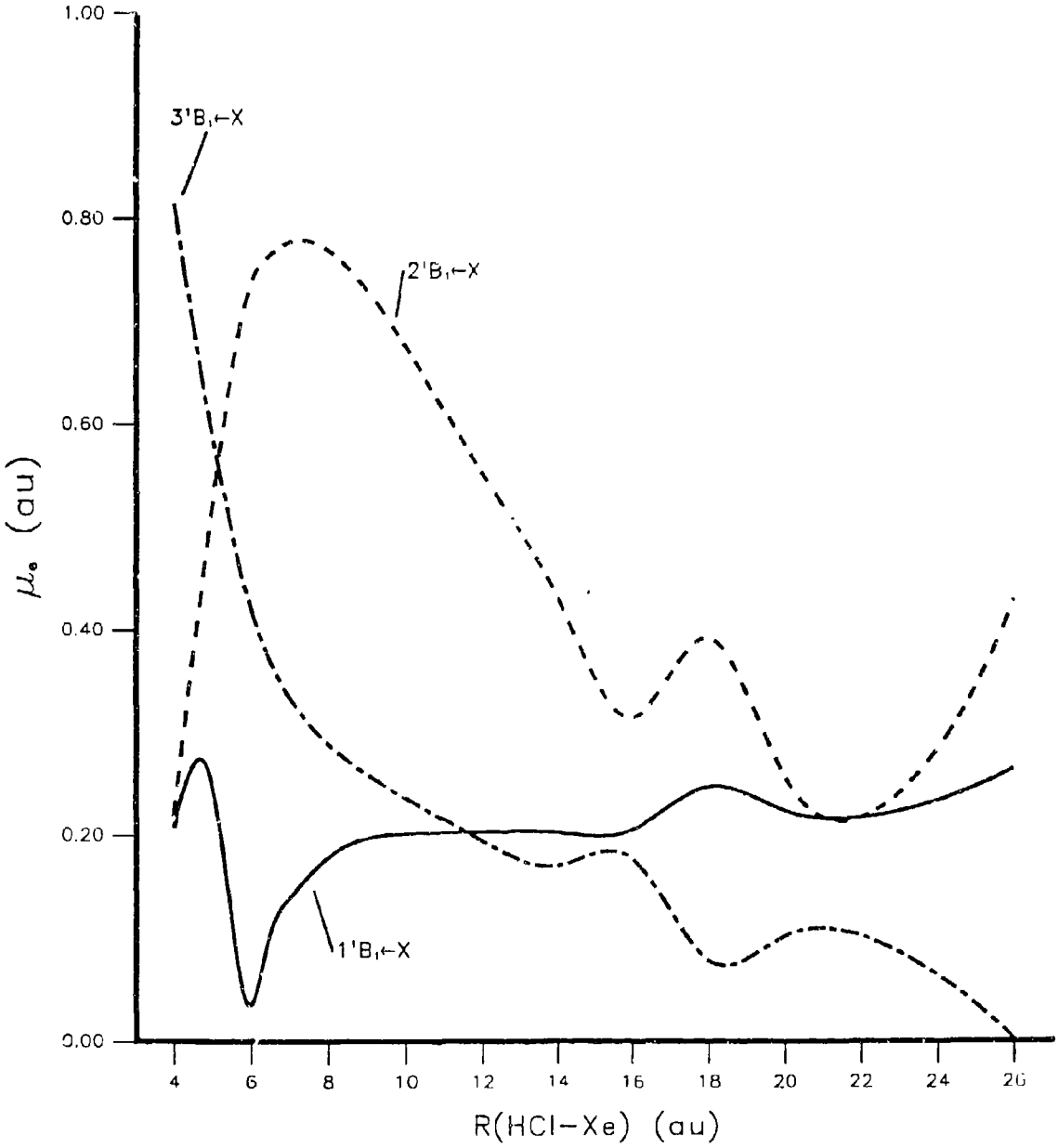

Figure 5. Absolute value of the electric dipole transition moment, μ_e (in atomic units), for the transitions from the ground state to the x-component of the three lowest lying singlet Π states belonging to the B_1 IRREP.

goes through zero (with a sign reversal) near R=6.0, and again rises to 0.18 at R=8.0. No attempt was made to verify the changes in sign for transition moments, since it would serve no purpose in this study. Examination of the CI coefficients for the main CSFs in the $1B_1$ and $2B_1$ states shows them exchanging character going from R=5.0 to 6.0, which probably accounts for the rapid change in the transition moment. From R=8.0, the moment slowly rises to a value of 0.27 at R=26.0, with a slight deviation from its monotonic increase occurring around R=18.0. At R=26.0, the transition moment appears to be approaching the values reported for the $\tilde{A}(^1\Pi)\leftarrow\tilde{X}$ transition in HCl, i.e. μ_e (HCl)=(0.37 [Adams and Chabalowski, to be published], 0.35–0.39 [Van Dishoeck, Van Hemert, and Dalgarno 1982]). Table 4 reports the transition dipole moments at selected points along the PECs, and Table 5 contains the permanent dipole moments for an expanded set of points on the PECs. It is interesting to look at the permanent dipole moment of the $1B_1$ along the PEC. From Table 5 we see it holds rather constant at values ranging from approximately 2 to 3 Debye for R ≥ 6.0. These values are in close agreement with the calculated value of +2.9 D (Adams and Chabalowski, to be published) for HCl in its $\tilde{A}(^1\Pi)$ state. A look at the vertical transition energies, T, for selected R-values given in Table 6 show T decreasing from 8.32 eV at R=6.0 to 8.04 eV at R=26.0, again in reasonable agreement with the T_e=(7.90 [Adams and Chabalowski, to be published], 7.84 [Bettendorff, Peyerimhoff, and Buenker 1982]) eV reported for the $\tilde{A}(^1\Pi)\leftarrow\tilde{X}$ transition in HCl.

Based on the transition energies and the permanent and transition dipole moments in the region R=8.0–20.0, the $1B_1$ state might best be described as the $\tilde{A}(^1\Pi)$ state in HCl moderately perturbed by the xenon. For R < 8.0, the xenon atom begins to have a significant affect on the properties, which is reasonable since the sum of van der Waal's radii for Cl(1.8 Å) and Xe(2.2 Å) is 7.6 bohr (4.0 Å). The transition moment shown in Figure 5 appears to be most strongly affected by the close proximity of the two species. The calculated properties for this state leads one to conclude that its character is that of the valence $\tilde{A}(^1\Pi)$ excited state of HCl perturbed by the Xe. Only at R=26.0 does this state truly become localized to HCl, and so only at R=26.0 can the $1B_1\leftarrow\tilde{X}$ transition be unambiguously assigned to the $\tilde{A}(^1\Pi)\leftarrow\tilde{X}$ transition in HCl.

4.1.2 The $2B_1$ State. At R=26.0, the $2B_1$ is described as a $Cl(p_x)\rightarrow\sigma^*(HCl)$ excitation, with the AOs on Xe making a very little contribution to the singly occupied MOs in the main CSFs. The transition energy given in Table 6 for R=26.0 bohr is T=9.93 eV, which lies reasonably close to T_e=(9.65 [Adams and Chabalowski 1993], 9.67 [Bettendorff, Peyerimhoff, and Buenker 1982]) for the $\tilde{C}(^1\Pi)\leftarrow\tilde{X}$ Rydberg transition in HCl. The values reported in Table 4 for the transition dipole moment in HCl are μ_e=(0.57)

Table 4. Absolute Values of the Electric Dipole Transition Moments, μ_e, Between the Ground $\tilde{X}(^1A_1)$ and Excited States at Selected R(HCl•••Xe) Distances

	μ_e[a]					
State[b]	R=6.0[c]	R=8.0	R=12.0	R=18.0	R.26.0	HCl
2^1A_1	0.69	0.68	0.75	0.18	0.01	
3^1A_1	1.01	0.34	0.12	0.05	0.00	
1^1B_1	0.04	0.18	0.20	0.25	0.27	0.37,[d] 0.35–0.39[e]
2^1B_1	0.74	0.77	0.55	0.39	0.43	0.57,[d] 0.48[e]
3^1B_1	0.42	0.29	0.19	0.08	0.00	

[a] Transition dipole moments are in atomic units.
[b] Transitions to the B_1 states represent only the Π_x component.
[c] R is the distance, in bohrs, between Cl and Xe.
[d] Adams and Chabalowski (to be published), for R(H-Cl)=2.40 bohr.
[e] van Dishoeck et al. for R(H-Cl)=2.41 bohr.

Table 5. Permanent Electric Dipole Moments at Selected R Values for the Six Electronic States in This Study

	Permanent Electric Dipole Moments (Debye)					
R(bohr)	$1A_1$	$2A_1$	$3A_1$	$1B_1$	$2B_1$	$3B_1$
4.0	-0.62	+1.55	+0.07	+1.09	+6.79	+0.10
5.0	-1.40	-0.92	+11.61	+1.65	+1.00	-6.46
6.0	-1.53	-0.63	+15.88	+3.09	-0.54	-12.34
6.4	-1.53	+0.04	+17.36	+2.99	+0.08	-13.37
7.0	-1.52	+1.11	+19.10	+2.83	+1.14	-14.17
8.0	-1.50	+3.15	+21.92	+2.15	+3.19	-14.86
10.0	-1.49	+7.25	+27.60	+2.35	+7.31	-15.72
12.0	-1.50	+11.07	+33.20	+2.35	+11.13	-16.88
14.0	-1.50	+15.53	+38.42	+2.39	+15.57	-17.57
16.0	-1.51	+21.82	+43.18	+2.37	+21.85	-16.73
18.0	-1.52	+37.09	+47.51	+2.22	-7.38	+37.20
20.0	-1.51	+39.89	+51.76	+2.29	-10.53	+39.96
26.0	-1.54	+64.49	+67.38	+2.65	-2.85	+64.52

NOTE: A positive dipole moment is defined as having the positive end of the vector pointing toward the Xe atom.

Table 6. Vertical Transition Energies, T, Between the Ground $\tilde{X}$ ($^1A_1$) and Excited States at Selected R(HCl•••Xe) Distances

	T (eV)				
State	R=6.0[a]	R=8.0[b]	R=18.0	R=26.0	HCl
2^1A_1	8.60	8.90	10.81	11.47	
3^1A_1	10.81	11.82	13.86	14.48	
1^1B_1	8.32	8.23	8.07	8.04	7.90,[c] 7.84[d]
2^1B_1	8.75	8.89	9.96	9.93	9.65,[c] 9.67[d]
3^1B_1	10.39	10.70	10.84	14.53	

[a] R is the distance, in bohrs, between Cl and Xe.

[b] Cl-Xe distance corresponding to lowest energy calculated for the $\tilde{X}(1A_1)$ ground state.

[c] Adams and Chabalowski (to be published), for R(H-Cl)=2.43 bohr.

[d] Bettendorff, Peyerimhoff, and Buenker (1982), for R(H-Cl)=2.40 bohr.

[Adams and Chabalowski, to be published], 0.48 [Van Dishoeck, Van Hemert, and Dalgarno 1982]), to be compared with the current value of μ_e(R=26.0)=0.43 atomic units. Previous ab initio CI calculations (Adams and Chabalowski, to be published) on HCl predict the permanent dipole moment for the $\tilde{C}(^1\Pi)$ state to be -0.74 D, to be compared with the current value of -2.8 at R=26.0. Even though the value for HClXe is almost three times that of HCl, they are both relatively small dipole moments and both negative. The $2B_1$ state has the only negative permanent dipole of the three B_1 states at R=26.0. The HCl and Xe seem to have a rather long-range interaction as can be seen in the changing permanent dipole in Table 7, as well as the transition dipole moments in Figure 5, even as R increases beyond 20 bohr (~10.6 Å). So at R=26.0, the $2B_1$ electronic state does appear to be Rydberg in its extensiveness. This, coupled with the calculated properties, suggests that, at R=26.0, the $2B_1$ correlates with the $\tilde{C}(^1\Pi)\leftarrow\tilde{X}$ Rydberg transition in HCl slightly perturbed by the Xe atom.

It is now interesting to examine the rather large changes in properties as the Xe approaches the HCl. In Figure 5, the transition moment shows irregular behavior in moving from R=26 to 16 bohr, particularly in the region R=16-20. From the PECs in Figure 4, it appears that the $2B_1$ encounters avoided crossings with other B_1 states in this region, explaining the peculiar behavior of the transition moments in this region. Beginning with μ_e=0.31 atomic units at R=16, the transition moment increases as R decreases, reaching a maximum of μ_e=0.78 atomic units at R=7.0, and finally decreasing to 0.22 at R=4.0. The

vertical transition energy, T=8.89 eV, at R=8.0 (see Table 6) show this transition to be separated from the $1B_1 \leftarrow 1A_1$ transition by only 0.66 eV. This is considerably less than the separation between the $\tilde{C} \leftarrow \tilde{X}$ and $\tilde{A} \leftarrow \tilde{X}$ transitions in HCl, i.e., ΔT_e=1.75 eV, to which these two transitions appear to correlate at dissociation. One interpretation of this would be that the xenon atom preferentially stabilizes the $\tilde{C}$ state over the $\tilde{A}$ state in HCl. It is also worth noting the depth of the lower minimum in the double-well potential shown for this state at R_e=7.04 in Figure 4. If we define the barrier to dissociation to be $\Delta E^* = T_{Re} - T_{R=20.0}$, then ΔE^*=1.65 eV (37.9 kcal/mol), which is a fairly sizable barrier to dissociation. The permanent dipole moment is calculated to be +3.2 D at R=8.0, similar to the $1B_1$ state and much too small to be considered as an electron transfer state. In summary, for the region R=6.0–20.0 the main CSFs for $2B_1$ show it to be a state composed of electron density from both Cl and Xe, hence having no counterpart in the isolated Xe or HCl. But at the largest R value treated here, R=26.0 bohr, the $2B_1$ state becomes a $\pi \rightarrow \sigma^*$ transition located primarily on the HCl and roughly correlates with the $\tilde{C} \leftarrow \tilde{X}$ Rydberg transition in HCl slightly perturbed by the xenon.

4.1.3 The $3B_1$ State. At R=26.0 bohr, this state is predicted to lie 14.53 eV above the ground state. The earlier theoretical studies on HCl (Bettendorff, Peyerimhoff, and Buenker 1982; Van Dishoeck, Van Hemert, and Dalgarno 1982; Adams and Chabalowski, to be published) did not report excited electronic states at such high transition energies, but even if such high lying states had been reported, the $3B_1$ could not be associated with any HCl state due to its description in its main CSF. This CSF, with CI coefficient c^2=0.88, represents an electronic promotion from MO $1b_1$ into $5a_1$, where $1b_1$ is essentially the Xe(p_x) AO and $5a_1$ is essentially the Cl(s–Rydberg) AO. This state then represents an ionic or electronic transfer state of Π symmetry. One can substantiate this claim by examining the permanent dipole moments given in Table 5. Its value at R=26.0 is +64.5 D, which obviously makes this a very polar state. But if we look at the transition dipole moment (Table 4) at R=26.0, we see that there is essentially zero probability for this electron transfer to occur. The excitation probability does increase as R decreases, such that at R=16.0 the transition moment is calculated to be 0.18 atomic units, and the transition energy has dropped to ~11 eV, while the permanent dipole moment still remains very large but of opposite sign at -16.73 D. This change in sign of the permanent dipole moment in going from R=18.0 to 16.0 indicates a radical change in the character of the $3B_1$ state, supporting the earlier statement that the PECs for the B_1 states show avoided crossings with one another in this region.

For distances around R=8.0, the state is still seen to be charge transfer in nature with a dipole moment of -14.9 D. It is interesting that the positive end of the dipole vector now points towards the hydrogen

atom and not the xenon. This would suggest electron transfer from the chlorine (or HCl) toward the xenon. A look at the main CSFs for the $3B_1$ over the entire PEC shows that this state, like the $2B_1$, is truly a state that exists due to the complex. The large and relatively steady decrease in the absolute magnitude of the transition moment from R=6.0 to R=14.0 supports the claim that the $3B_1$ state does not correlate closely with any state in the isolated species over any part of the PEC.

4.2 The $^1A_1$ States. All the $^1A_1$ states calculated here are predicted to be bound, although the ground state $1A_1$ is predicted to have a barrier to dissociation of only ~0.035 eV calculated from R_e=8.36 bohr. The semi-empirical calculations of Last and George (1988) predict an R_e(HCl---Xe) of 7.22 bohr with an H-Cl bond length of 2.41 bohr in the linear HClXe ground state complex. The potential well, however, is predicted to very shallow and broad as previously noted by Last and George (1988) and supported by this work as shown in Figure 6. Based on the level of theory used here, it is not possible to conclude whether or not the ground state is indeed bound. No efforts were made to correct for the basis set superposition error due to the qualitative nature of this study. The calculated D_e's for all the states are listed in Table 7. Both the 2 and 3^1A_1 states are described primarily by electronic promotions from the $4a_1$ MO of σ symmetry comprised almost entirely of atomic p_z density on the Xe atom into the $5a_1$ and $6a_1$ σ^* MOs. These are the same σ^* MOs involved in the $\pi \rightarrow \sigma^*$ excitations describing the main CSFs in the $^1B_1$ states.

4.2.1 The $2A_1$ State. The dominant CSF in the $2A_1$ wave function for R=6.0 to 16.0 bohr is a $4a_1 \rightarrow 5a_1$ single excitation. The square of the CI coefficient for this CSF is constant at c^2=0.86 over this region. This represents an electron promoted from an MO comprised essentially of the Xe(p_z) atomic orbitals into the $5a_1$ σ^* MO. Table 5 shows that the permanent electric dipole moment of the $2A_1$ state is nearly identical with the $2B_1$ state for R≥6.4–16.0, and Figure 7 shows the two PECs to be essentially degenerate over the region R=8.0 to 16.0 bohr. The similarities between these two states can be rationalized in terms of the sum of the van der Waals radii for Cl + Xe which is predicted to be 7.6 bohr for the electronic ground state of HClXe. As Cl approaches Xe along the z axis, the electron clouds for the two atoms should begin penetrating one another around 7.6 bohr. To a rough approximation, outside this distance the $4a_1$ MO can be thought of as a perturbed Xe(p_z) atomic orbital. In the $2B_1$ state, the electronic excitation arises primarily from the $1b_1$ (π_x) MO which is described predominantly by the Xe(p_x) atomic orbital for R>8.0. Thus, if the spherical symmetry of the xenon atom is only moderately perturbed by HCl, an excitation out of the $4a_1$ MO (i.e., Xe[p_z] AO) should be nearly indistinguishable

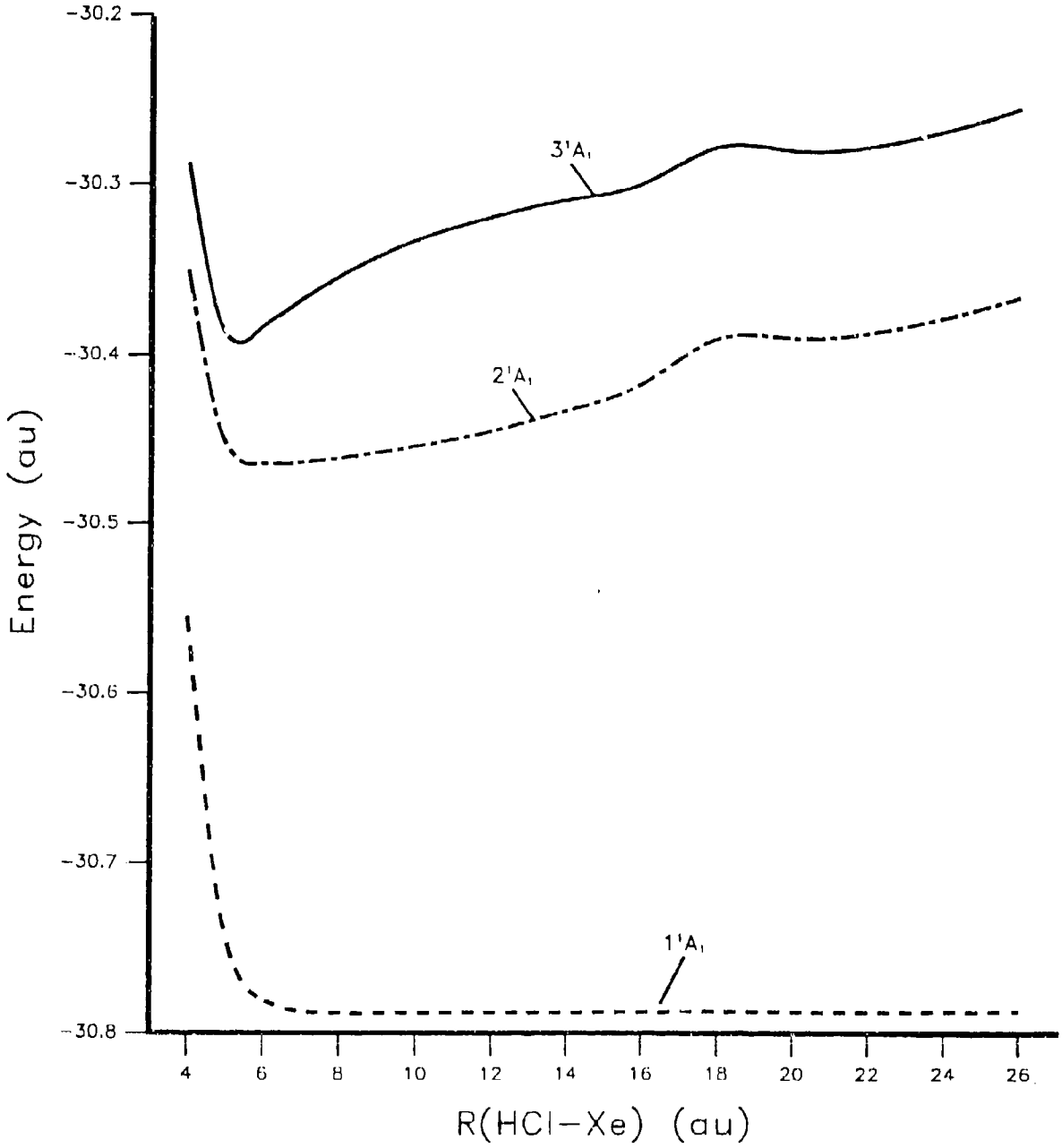

Figure 6. Potential energy curves for the three lowest $^1\Sigma^+$ electronic states belonging to the A_1 IRREP in linear HClXe. (See the text in section 4.2 for a detailed discussion of these states.)

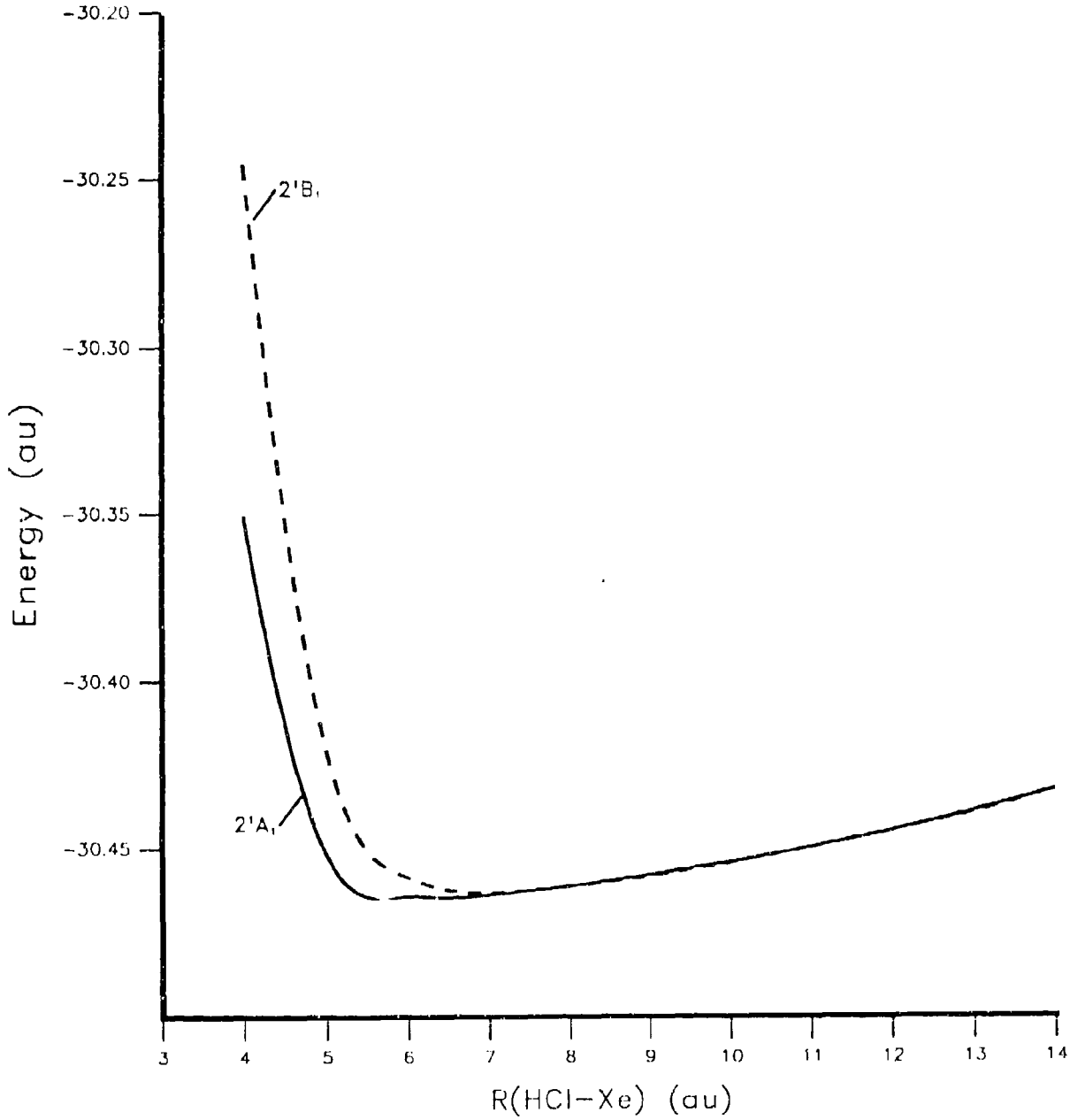

Figure 7. Potential energy curves for the $2A_1$ and $2B_1$ electronic states in linear HClXe. (See section 4.2.1 for a discussion of these PECs.)

Table 7. Calculated D_e's for HClXe[a]

State	D_e(eV)
1^1A_1	0.035
2^1A_1	2.7
3^1A_1	3.6
1^1B_1	—[b]
2^1B_1	1.1
3^1B_1	0.93

[a] D_e=E(4=8.0) - E(R=26.0), with R being the Cl-Xe separation in bohrs.
[b] Has a barrier to dissociation of 0.02 eV at R=16.0 bohr, but predicted to be unbound by definition of D_e given in footnote a.

from an excitation out of the $1b_1(\pi_x)$ MO (i.e., Xe[p_x] AO) as is the case for the $2B_1$ state. (The reader is reminded that both the A_1 and B_1 states are characterized by excitations into the same two σ^* MOs.) Hence, the PECs for the $2A_1$ and $2B_1$ begin to split apart (see Figure 7) for distances less than the sum of van der Waal's radii which is near ~8 bohr.

Between R=5.5 and 7.0 bohr, the $2A_1$ acts as if it is being preferentially stabilized over the $2B_1$ state by the approach of the Cl and Xe atoms. The permanent dipole moment in the region R=8.0–16.0 (+3.2 and +21.8 D at R=8.0 and 16.0, respectively) is too small for this to be considered a charge transfer state, however, one might interpret it as a Rydberg state polarized by the electro-negativity of the Cl atom. The transition moment remains large and rather constant, with values of μ_e^x=0.69 atomic units at R=6.0 bohr to 0.57 at R=16.0. The fact that the transition moment remains both constant and large over such a distance also supports the interpretation of this as a Rydberg state. For values of R≥10.0 bohr, the $ta_1(\sigma^*)$ has a significantly larger contribution from the Xe s-type AOs than any AOs on HCl. For these larger separations, the state resembles an Xe $p_z \rightarrow \sigma(s)$ Rydberg state of the xenon atom strongly perturbed by the HCl.

In the region R=18.0–20.0, there are apparently avoided crossings occurring amongst the A_1 excited states, having a significant effect on the energies (see Figure 6), permanent dipole moments, and transition dipole moments (see Figure 8). Finally, at R=26.0 bohr, the wave function is described by a CSF representing an electron promoted from the Xe(p_z) AOs into the Rydberg $\sigma(s)$ MO comprised almost

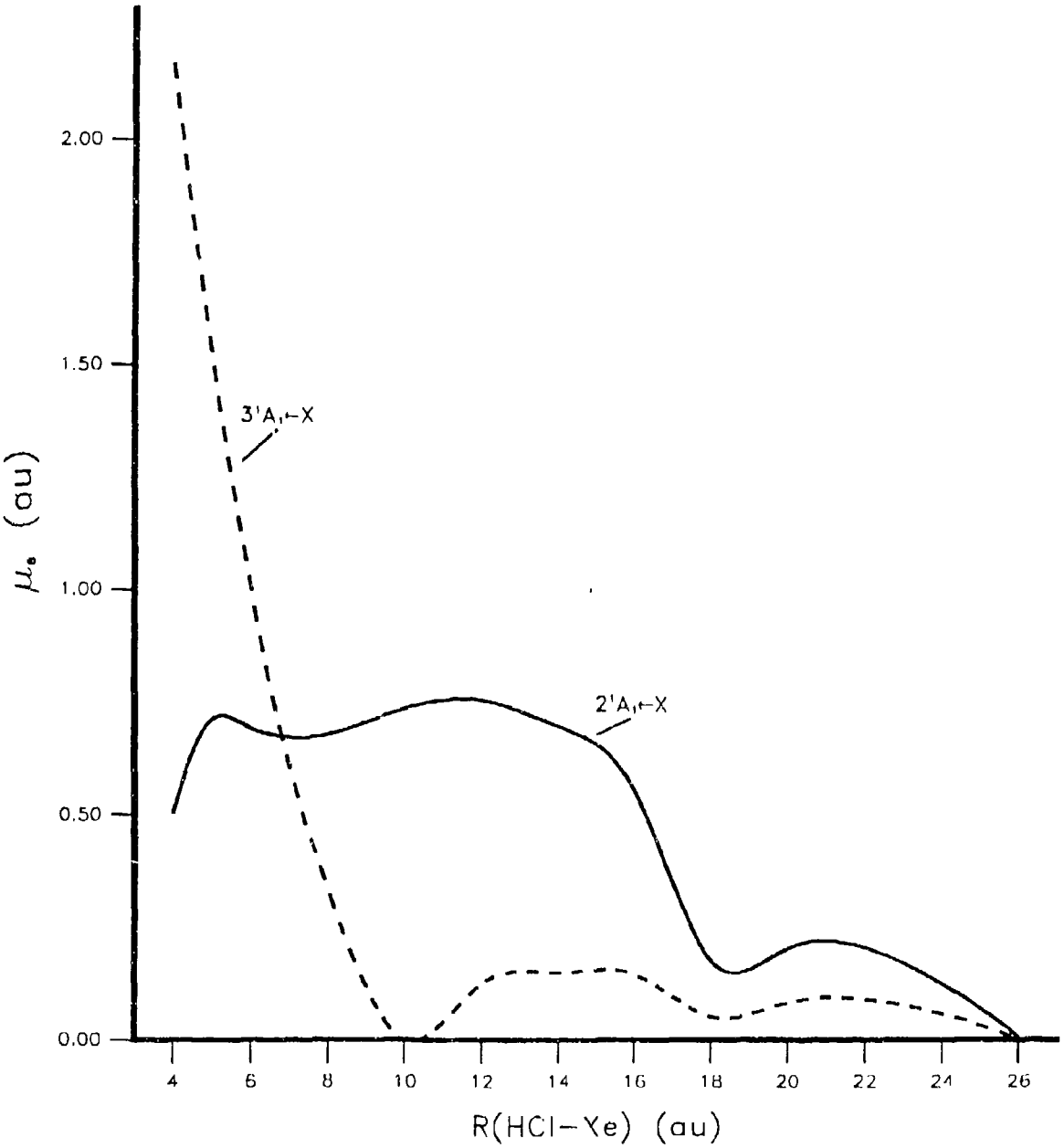

Figure 8. Absolute value of the electric dipole transition moment, μ_o (in atomic units), for the transitions from the ground state to the lowest lying $^1\Sigma^+$ excited states belonging to the A_1 IRREP.

entirely of Cl s-type AOs. The permanent dipole moment is +64 D, which is roughly the value of unit positive and negative charges separated by 26 bohr. This now appears to be a charge transfer state, however, the probability for reaching this state from the ground state is practically zero due to a vanishing transition dipole moment.

4.2.2 The $3A_1$ State. The 3^1A_1 resembles a true charge transfer state. This is substantiated by the value of the permanent dipole moment. At R=8.0, the dipole is predicted to be +21.9 D, while two unit point charges of opposite sign separated by 8.0 bohr would have a dipole moment of +20.3 D. The R_e is predicted to be 5.35 bohr, in good agreement with the bond length for the "4i" ionic state calculated to be R_e=5.52 bohr by Last and George (1988). It should be noted that their HCl bond length was allowed to vary in their optimization and was predicted to be 2.99 bohr, which is 0.58 bohr longer than the fixed bond length of R(HCl)=2.41 used here. The vertical transition energy at R=5.0 is T=9.62 eV, while T_e=10.86 eV calculated with R_e=5.35 for the $3A_1$. This can be compared to Last and George's value of T_e=8.43 eV, taken between the analogous minimum energy structures. Again it should be pointed out that our predicted T_e for the $3A_1$ state is undoubtedly too high due to having fixed the H–Cl bond length at 2.41 bohr. At R=5.0, this state is primarily described by a CSF defined as a single excitation $4a_1 \rightarrow 6a_1$, σ^* state. This represents an electronic excitation from the Xe p_z atomic AOs into an MO localized mostly on the HCl and having H-Cl σ-antibonding character. This would suggest a longer bond length for the H-Cl in this state, consistent with the results of Last and George (1988).

As R increases, the $3A_1$ state soon becomes the highest lying vertical transition calculated in this study, with T=11.82 eV at R=8.0. The transition energy steadily increases (except at R=20.0, see Table 6) to 14.48 eV at R=26.0 bohr. The $3A_1 \leftarrow \tilde{X}$ transition is calculated to be very intense for R≤7.0. The transition dipole moment drops rapidly from a value of μ_e=2.17 atomic units at R=4.0 to μ_e=0.0 at R=10.0 (see Figure 8). Along with the changing μ_e, the character of the $6a_1$ MO changes from one arising from density on HCl to one with contributions from all three atoms as R goes from 6 to 16 bohr. In the region of avoided crossings around R=18–20.0, the transition moment is seen to be small and finally drops to essentially zero at R=26.0.

This type of state, at least in the region R=6.0–8.0 bohr, could serve as a model for studying the charge transfer excitation in solid xenon matrices doped with HCl as reported by Apkarian and coworkers (Fajardo and Apkarian 1986; 1987; 1988a; 1988b; Schwentner, Fajardo, and Apkarian 1989; Wiedeman, Fajardo, and Apkarian 1987). As mentioned in the introduction, the Cl-Xe distance has been estimated

to be ~6.4 bohr in the gas phase $4^2\Gamma$ state of the charge transfer exciplex Xe_2Cl. These calculations predict a large probability of charge transfer in the $3A_1$ for R≈6.0–8.0 bohr based upon the calculated transition dipole and permanent dipole moments. This might then be followed by dissociation of HCl due to the H-Cl σ^*–antibonding character of the $6a_1$ MO which places a major role in describing the $3A_1$ state.

5. CONCLUSIONS

It has been shown that much insight into the XeCl interactions can be achieved through the combination of effective core potentials and wave functions obtained from state average MCSCF and CI calculations. The results on XeCl compare favorably with earlier ab initio work by Hay and Dunning (1978), but it is clear that the spin-orbit corrections now available to us will be indispensable for attaining quantitative accuracy in predicting transition energies and transition strengths.

The results of the HCl-Xe calculations have produced much insight into the fundamental nature of the excited states in this system. The 1 and 2^1B_1 states are predicted to look like molecular HCl states perturbed by the Xe atom at values of R(HCl-Xe) less than 10 bohr. At dissociation, these states closely resemble the $\bar{A}(^1\Pi)$ and $\bar{C}(^1\Pi)$ states of HCl plus a ground state Xe atom. In contrast, the 3^1B_1 state shows characteristics associated with the HClXe molecule as a whole, represented by an electron promotion of π(XeCl)→σ(HClXe).

The 2^1A_1 state also shows characteristics associated with the entire HClXe molecule. But the 3^1A_1 state is by far the most interesting and clearly represents a charge transfer state with a transfer of an electron from the Xe atom to an antibonding σ(HCl) MO, just as predicted from the experiments of Apkarian and coworkers in the halogen-doped xenon (and other Rg) matrices.

6. REFERENCES

Adams, G. F., and C. F. Chabalowski. "Quantum Chemical Study of Rare Gas/Halide Interactions as a Model for High Energy Density Material: I. Transition Properties in HCl." U.S. Army Research Laboratory Research Report, Aberdeen Proving Ground, MD, to be published.

Alimi, R., A. Brokman, and R. B. Gerber. "Molecular Dynamics Simulations of Reactions in Solids: Photodissociation of Cl_2 in Crystalline Xe." Journal of Chemical Physics, vol. 91, p. 1611, 1989.

Alimi, R., R. B. Gerber, and V. A. Apkarian. "Dynamics of Molecular Reactions in Solids: Photodissociation of HI in Crystalline Xe." Journal of Chemical Physics, vol. 89, p. 174, 1989.

Alimi, R., R. B. Gerber, and V. A. Apkarian. "Dynamics of Molecular Reactions in Solids: Photodissociation of F_2 in Crystalline Ar." Journal of Chemical Physics, vol. 92, p. 3551, 1990.

Bettendorff, M., S. D. Peyerimhoff, and R. J. Buenker. "Clarification of the Assignment of the Electronic Spectrum of Hydrogen Chloride Based on Ab Initio Calculations." Chemical Physics, vol. 66, p. 261, 1982.

Brau, C. A., and J. J. Ewing. "Emission Spectra of XeBr, XeCl, XeF, and KrF." Journal of Chemical Physics, vol. 63, p. 4640, 1975.

Chabalowski, C. F., J. O. Jensen, D. R. Yarkony, and B. H. Lengsfield. "Theoretical Study of the Radiative Lifetime for the Spin-Forbidden Transition $a^3\Sigma_u \rightarrow X^1\Sigma_g$ in He_2." Journal of Chemical Physics, vol. 90, p. 2504, 1989.

Dunning, T. H., and P. J. Hay. Methods of Electronic Structure Theory: Modern Theoretical Chemistry, vol. 3. Edited by H. F. Schaefer III. New York: Plenum Press, chap. 1, pp. 1–28, 1977.

Fajardo, M. E., and V. A. Apkarian. "Cooperative Photoabsorption Induced Charge Transfer Reaction Dynamics in Rare Gas Solids. I. Photodynamic of Localized Xenon Chloride Exciplexes." Journal of Chemical Physics, vol. 85, p. 5660, 1986.

Fajardo, M. E., and V. A. Apkarian. "Stimulated Radiative Dissociation and Gain Measurements of Xe_2Cl in Solid Xenon." Chemical Physics Letters, vol. 134, p. 51, 1987.

Fajardo, M. E., and V. A. Apkarian. "Charge Transfer Photodynamic in Halogen Doped Xenon Matrices. II. Photoinduced Harpooning and the Delocalized Charge Transfer States of Solid Xenon Halides (F, Cl, Br, I)." Journal of Chemical Physics, vol. 89, p. 4102, 1988a.

Fajardo, M. E., and V. A. Apkarian. " Energy Storage and Thermoluminescence in Halogen Doped Solid Xenon. III. Photodynamic of Charge Separation, Self-Trapping, and Ion-hole Recombination." Journal of Chemical Physics, vol. 89, p. 4124, 1988b.

Fajardo, M. E., V. A. Apkarian, A. Moustakas, J. Krueger, and E. Weitz. "Absorption Spectra of Intermolecular Charge-Transfer Transitions Between Xenon and Halogen Molecules (F_2, Cl_2, Br_2) in Liquid Xenon." Journal of Physical Chemistry, vol. 92, p. 357, 1988.

Gerber, R. B., R. Alimi, and V. A. Apkarian. "Ion Migration Following Charge Transfer Reactions in Rare-Gas Solids: The Role of Hole Hopping." Chemical Physics Letters, vol. 158, p. 257, 1989.

Grieneissen, M. P., H. Xue-Ting, and K. L. Komps. "Collision Complex Excitation in Chlorine-Doped Xenon." Chemical Physics Letters, vol. 82, p. 441, 1981.

Hay, P. J., and T. Dunning. "The Covalent and Ionic States of the Xenon Halides." Journal of Chemical Physics, vol. 69, p. 2209, 1978.

Huber, K. P., and G. Herzberg. Molecular Spectra and Molecular Structure: Constants of Diatomic Molecules, vol. 4, Princeton, NJ: Van Nostrand, 1979.

Inoue, G., J. K. Ku, and D. W. Setser. "Photoassociative Laser-Induced Fluorescence of XeeL* and Kinetics of XeCl(B) and XeCl(C) in Xe." Journal of Chemical Physics, vol. 80, p. 6006, 1984.

Katz, A. I., J. Feld, and V. A. Apkarian. "Solid-State Xe (D → X) Laser at 286 nm." Optics Letters, vol. 14, p. 441, 1989.

Kunttu, H., J. Feld, R. Alimi, A. Becker, and V. A. Apkarian. "Charge Transfer and Radiative Dissociation Dynamics in Fluorine-Doped Solid Krypton and Argon." Journal of Chemical Physics, vol. 92, p. 4856, 1990.

Last, I., and T. F. George. "Interaction of Xe^+ and Cl^- Ions and Their Formed Molecules With a Xe Solid Matrix." Journal of Chemical Physics, vol. 86, p. 3787, 1987a.

Last, I., and T. F. George. "Semiempirical Study of Polyatomic Rare Gas Halides: Application to the Xe_nCl Systems." Journal of Chemical Physics, vol. 87, p. 1183, 1987b.

Last, I., and T. F. George. "Electronic States of the Xe_nHCl Systems in Gas and Condensed Phases." Journal of Chemical Physics, vol. 89, p. 3071, 1988.

Last, I., T. F. George, M. E. Fajardo, and V. A. Apkarian. "Potential Energy Surfaces and Transition Moments of a Cl Atom in a Xe Solid Matrix." Journal of Chemical Physics, vol. 87, p. 5917, 1987.

Last, I., Y. S. Kim, and T. F. George. "Cooperative Optical Transitions in Impurity Centers Coupled Via Host Atoms." Chemical Physics Letters, vol. 138, p. 225, 1987.

Lengsfield, B. H. "General Second-Order MCSCF Theory for Large CI Expansions." Journal of Chemical Physics, vol. 77, p. 4073, 1982.

Liu, B., and M. Yoshimine. "The Alchemy Configuration Interaction Method. I. The Symbolic Matrix Method for Determining Elements of Matrix Operators." Journal of Chemical Physics, vol. 74, p. 612, 1981.

Okada, F., L. Wiedeman, and V. A. Apkarian. "Photoinduced Harpoon Reactions as a Probe of Condensed-Phase Dynamics: ICl in Liquid and Solid Xenon." Journal of Physical Chemistry, vol. 93, p. 1267, 1989.

Perry, J. K., and D. R. Yarkony. "On the Electronic Strucutre of the He + H_2 system: Characterization of, and Nonadiabatic Interactions Between, the $1^1A'$ and $2^1A'$ Potential Energy Surfaces." Journal of Chemical Physics, vol. 89, p. 4945, 1988.

Schwentner, N., and V. A. Apkarian. "A Solid State Rare Gas Halide Laser: XeF in Crystalline Argon." Chemical Physics Letters, vol. 154, p. 413, 1989.

Schwentner, N., M. E. Fajardo, and V. A. Apkarian. "Rydberg Series of Charge Transfer Excitations in Halogen-Doped Rare Gas Crystals." Chemical Physics Letters, vol. 154, p. 237, 1989.

Stevens, W. J., and M. Krauss. "Absorption in the Triatomic Excimer, Xe_2Cl." Applied Physics Letters, vol. 41, p. 301, 1982.

Van Dishoeck, E. F., M. C. van Hemert, and A. Dalgarno. "Photodissociation Processes in the HCl Molecule." Journal of Chemical Physics, vol. 77, p. 3693, 1982.

Van Duijneveldt, F. B. "Gaussian Basis Sets for the Atoms H-Ne for Use in Molecular Calculations." IBM Research Report RJ945, 10 December 1971.

Velazco, J. E., and D. W. Setser. "Bound-Free Emission Spectra of Diatomic Xenon Halides." Journal of Chemical Physics, vol. 62, p. 1990, 1975.

Wadt, W. R., and P. J. Hay. "Ab Initio Effective Core Potentials for Molecular Calculations. Potentials for Main Group Elements Na to Bi." Journal of Chemical Physics, vol. 82, p. 284, 1985.

Wiedeman, L., M. E. Fajardo, and V. A. Apkarian. "Cooperative Photoproduction of $Xe_2(+)Cl(-)$ in Liquid Cl_2/Xe Solutions: Stimulated Emission and Gain Measurements." Chemical Physics Letters, vol. 134, p. 55, 1987.

INTENTIONALLY LEFT BLANK.

NO. OF COPIES	ORGANIZATION
2	ADMINISTRATOR DEFENSE TECHNICAL INFO CENTER ATTN: DTIC-DDA CAMERON STATION ALEXANDRIA VA 22304-6145
1	COMMANDER US ARMY MATERIEL COMMAND ATTN: AMCAM 5001 EISENHOWER AVE ALEXANDRIA VA 22333-0001
1	DIRECTOR US ARMY RESEARCH LABORATORY ATTN: AMSRL-OP-SD-TA/ RECORDS MANAGEMENT 2800 POWDER MILL RD ADELPHI MD 20783-1145
3	DIRECTOR US ARMY RESEARCH LABORATORY ATTN: AMSRL-OP-SD-TL/ TECHNICAL LIBRARY 2800 POWDER MILL RD ADELPHI MD 20783-1145
1	DIRECTOR US ARMY RESEARCH LABORATORY ATTN: AMSRL-OP-SD-TP/ TECH PUBLISHING BRANCH 2800 POWDER MILL RD ADELPHI MD 20783-1145
2	COMMANDER US ARMY ARDEC ATTN: SMCAR-TDC PICATINNY ARSENAL NJ 07806-5000
1	DIRECTOR BENET LABORATORIES ATTN: SMCAR-CCB-TL WATERVLIET NY 12189-4050
1	DIRECTOR US ARMY ADVANCED SYSTEMS RESEARCH AND ANALYSIS OFFICE ATTN: AMSAT-R-NR/MS 219-1 AMES RESEARCH CENTER MOFFETT FIELD CA 94035-1000

NO. OF COPIES	ORGANIZATION
1	COMMANDER US ARMY MISSILE COMMAND ATTN: AMSMI-RD-CS-R (DOC) REDSTONE ARSENAL AL 35898-5010
1	COMMANDER US ARMY TANK-AUTOMOTIVE COMMAND ATTN: AMSTA-JSK (ARMOR ENG BR) WARREN MI 48397-5000
1	DIRECTOR US ARMY TRADOC ANALYSIS COMMAND ATTN: ATRC-WSR WSMR NM 88002-5502
1	COMMANDANT US ARMY INFANTRY SCHOOL ATTN: ATSH-WCB-O FORT BENNING GA 31905-5000
	ABERDEEN PROVING GROUND
2	DIR, USAMSAA ATTN: AMXSY-D AMXSY-MP/H COHEN
1	CDR, USATECOM ATTN: AMSTE-TC
1	DIR, USAERDEC ATTN: SCBRD-RT
1	CDR, USACBDCOM ATTN: AMSCB-CII
1	DIR, USARL ATTN: AMSRL-SL-I
5	DIR, USARL ATTN: AMSRL-OP-AP-L

NO. OF COPIES	ORGANIZATION
1	HQDA (SARD-TR/MS K KOMINOS) WASH DC 20310-0103
1	HQDA (SARD-TR/DR R CHAIT) WASH DC 20310-0103

NO. OF COPIES	ORGANIZATION
	ABERDEEN PROVING GROUND
35	DIR, USARL ATTN: AMSRL-WT-P/A W HORST AMSRL-WT-PC/ R A FIFER G F ADAMS W R ANDERSON R A BEYER S W BUNTE C F CHABALOWSKI K P CLEMENTS A COHEN R CUMPTON R DANIEL D DEVYNCK N F FELL B E FORCH J M HEIMERL A J KOTLAR M R MANAA W F MCBRATNEY K L MCNESBY S V MEDLIN M S MILLER A W MIZIOLEK S H MODIANO J B MORRIS J E NEWBERRY S A NEWTON R A PESCE-RODRIGUEZ B M RICE R C SAUSA M A SCHROEDER J A VANDERHOFF M WENSING A WHREN J M WIDDER C WILLIAMSON

USER EVALUATION SHEET/CHANGE OF ADDRESS

This Laboratory undertakes a continuing effort to improve the quality of the reports it publishes. Your comments/answers to the items/questions below will aid us in our efforts.

1. ARL Report Number ARL-TR-621 Date of Report November 1994

2. Date Report Received _____

3. Does this report satisfy a need? (Comment on purpose, related project, or other area of interest for which the report will be used.) _____

4. Specifically, how is the report being used? (Information source, design data, procedure, source of ideas, etc.) _____

5. Has the information in this report led to any quantitative savings as far as man-hours or dollars saved, operating costs avoided, or efficiencies achieved, etc? If so, please elaborate. _____

6. General Comments. What do you think should be changed to improve future reports? (Indicate changes to organization, technical content, format, etc.) _____

CURRENT ADDRESS

Organization

Name

Street or P.O. Box No.

City, State, Zip Code

7. If indicating a Change of Address or Address Correction, please provide the Current or Correct address above and the Old or Incorrect address below.

OLD ADDRESS

Organization

Name

Street or P.O. Box No.

City, State, Zip Code

(Remove this sheet, fold as indicated, tape closed, and mail.)
(DO NOT STAPLE)